

# Preparation and antibacterial activity of chitosan nanoparticles

Lifeng Qi,\* Zirong Xu, Xia Jiang, Caihong Hu and Xiangfei Zou

Zhejiang University, Animal Science College, Key Laboratory of Molecular Animal Nutrition,  
Ministry of Education, Hangzhou 310029, China

Received 26 February 2004; accepted 6 September 2004

Available online 12 October 2004

**Abstract**—Chitosan nanoparticles, such as those prepared in this study, may exhibit potential antibacterial activity as their unique character. The purpose of this study was to evaluate the *in vitro* antibacterial activity of chitosan nanoparticles and copper-loaded nanoparticles against various microorganisms. Chitosan nanoparticles were prepared based on the ionic gelation of chitosan with triphosphate anions. Copper ions were adsorbed onto the chitosan nanoparticles mainly by ion-exchange resins and surface chelation to form copper-loaded nanoparticles. The physicochemical properties of the nanoparticles were determined by size and zeta potential analysis, atomic force microscopy (AFM), FTIR analysis, and XRD pattern. The antibacterial activity of chitosan nanoparticles and copper-loaded nanoparticles against *E. coli*, *S. choleraesuis*, *S. typhimurium*, and *S. aureus* was evaluated by calculation of minimum inhibitory concentration (MIC) and minimum bactericidal concentration (MBC). Results show that chitosan nanoparticles and copper-loaded nanoparticles could inhibit the growth of various bacteria tested. Their MIC values were less than 0.25 µg/mL, and the MBC values of nanoparticles reached 1 µg/mL. AFM revealed that the exposure of *S. choleraesuis* to the chitosan nanoparticles led to the disruption of cell membranes and the leakage of cytoplasm.

© 2004 Elsevier Ltd. All rights reserved.

**Keywords:** Chitosan nanoparticles; Copper-loaded nanoparticles; Antibacterial activity; AFM

## 1. Introduction

Chitosan is a natural nontoxic biopolymer derived by the deacetylation of chitin. Chitosan and its derivatives have attracted considerable interest due to their antimicrobial and antifungal activity.<sup>1–3</sup> Chitosan exhibits its antibacterial activity only in an acidic medium because of its poor solubility above pH 6.5.<sup>4</sup> The antibacterial activity of chitosan is influenced by a number of factors that include the type of chitosan, the degree of chitosan polymerization and some of its other physicochemical properties. Chitosan exhibits higher antibacterial activity against Gram-positive bacteria than Gram-negative bacteria. The antibacterial activity of chitosan also depends on the molecular weight and solvent,<sup>5</sup> and is inversely affected by pH, with higher activity at lower pH values.<sup>6</sup>

Chitosan is a mucoadhesive polymer that is able to open tight junctions and allow the paracellular transport of molecules across mucosal delivery of vaccines.<sup>7</sup> Chitosan microparticles and nanoparticles loaded with DNA plasmids were reported to induce protective immune responses in mice.<sup>8,9</sup>

Chitosan nanoparticles have been synthesized as drug carriers as reported in previous studies.<sup>10–12</sup> Insulin-loaded chitosan nanoparticles could enhance intestinal absorption of insulin and increase its relative pharmacological bioavailability.<sup>13</sup> Chitosan nanoparticles had also been employed as a gene carrier to enhance gene-transfer efficiency in cells.<sup>14,15</sup> Chitosan microspheres have been used for gastric drug delivery. Reacetylated chitosan microspheres have been prepared for controlled release of active antimicrobial agents, such as amoxicillin and metronidazole in the gastric cavity.<sup>16</sup> However, the antibacterial activity of chitosan nanoparticles has only seldom been reported elsewhere. The unique character of nanoparticles for their small size

\* Corresponding author. Tel.: +86 571 86971075; fax: +86 571 86091820; e-mail: [lfqi@zju.edu.cn](mailto:lfqi@zju.edu.cn)

and quantum size effect could make chitosan nanoparticles exhibit superior activities.

Chitosan nanoparticles and copper-loaded nanoparticles were prepared based on the ionic gelation of chitosan with tripolyphosphate anions. Their antibacterial activities against various microorganism were studied. The morphological changes of *S. choleraesuis* treated with chitosan nanoparticles were examined by atomic force microscopy (AFM).

## 2. Experimental

### 2.1. Materials

Chitosan was obtained from the Chitosan Company of Pan'an (Zhejiang Province, China) and refined twice by dissolving it in dilute HOAc solution. The solution was filtered, the chitosan was precipitated with aqueous sodium hydroxide, and the precipitate was dried in vacuum at room temperature.<sup>17</sup> The degree of deacetylation was about 85% as determined by elemental analysis, and the average molecular weight of the chitosan was 220 kDa as determined by viscometric methods.<sup>18</sup> Tripolyphosphate and doxycycline were supplied by Sigma Chemical Co. (USA). *E. coli* K88, *E. coli* ATCC 25922, *S. choleraesuis* ATCC 50020, *S. typhimurium* ATCC 50013, and *S. aureus* ATCC 25923 were provided by the Epidemic Prevention Center of Zhejiang Province, China, and stored at 4°C.

### 2.2. Preparation of chitosan nanoparticles and copper-loaded nanoparticles

Chitosan was dissolved at 0.5% (w/v) with 1% (v/v) HOAc and then raised to pH 4.6–4.8 with 10N NaOH. Chitosan nanoparticles formed spontaneously upon addition of 1 mL of an aqueous tripolyphosphate solution (0.25%, w/v) to 3 mL of chitosan solution under magnetic stirring. Nanoparticles were purified by centrifugation at 9000g for 30 min. Supernatants were discarded, and the chitosan nanoparticles were extensively rinsed with distilled water to remove any sodium hydroxide and then freeze-dried before further use or analysis. Copper-loaded chitosan nanoparticles were obtained by adding a solution of copper ions (100 µg/mL) to the chitosan nanoparticle suspension (0.375%, w/v) before purification. The purification was then carried out as for the chitosan nanoparticles described above.

### 2.3. Characterization

Chitosan, chitosan nanoparticles, and copper-loaded nanoparticles were characterized by following measurements.

Particle size distribution and the zeta potential of chitosan nanoparticles were determined using Zetasizer Nano-ZS90 (Malvern Instruments). The analysis was performed at a scattering angle of 90° at a temperature of 25°C using samples diluted to different intensity concentration with de-ionized distilled water. FTIR spectra of chitosan nanoparticles were taken with potassium bromide pellets on a Nicolet Nexus 670 spectrometer.

Atomic force microscopy (AFM, SPM-9500J3) was used for visualization of both the chitosan nanoparticles and copper-loaded nanoparticles deposited on silicon substrates operating in the contact mode. AFM imaging was performed using Si<sub>3</sub>N<sub>4</sub> probes with a spring constant of 0.06 N/m. X-ray powder diffraction patterns of chitosan nanoparticles were obtained by a D/max-rA diffractometer. The X-ray source was CuKα radiation (40 kV, 80 mA). Samples were scanned at a scanning rate of 4°/min.

### 2.4. Assays for antibacterial activity

The minimum inhibitory concentration (MIC) of chitosan and chitosan nanoparticles was determined by a turbidimetric method.<sup>19</sup> In this method, a number of test tubes each containing 5.0 mL of Muller–Hinton broth (MHB, Difco, England) were autoclaved for 15 min at 121°C. Chitosan is only soluble in acetic media, while chitosan nanoparticles could be well distributed in distilled water medium for its nice dispersity. Chitosan or chitosan nanoparticles powder was accurately quantified and added to distilled water or 0.25% acetic acid. The pH of the samples in suspension in distilled water was about 6.5, while that of one in 0.25% acetic acid was about 5.0. To the first tube, 5.0 mL of chitosan solution or chitosan nanoparticles (1 mg/mL) suspension was added. After mixing, 5.0 mL of the mixture was transferred to the second tube, and similar transformations were repeated. Hence, each tube contained a test sample solution with half of the concentration of the previous one. The tubes were inoculated under aseptic conditions with 50 µL of the freshly prepared bacteria suspension. The positive control was given with doxycycline, and the blank control tubes were only contained Muller–Hinton broth and 0.25% acetic acid. After mixing, the tubes were incubated at 37°C for 24 h. The tubes were then studied for the visible signs of growth or turbidity. The lowest concentration of chitosan and nanoparticles that inhibited the growth of bacteria was considered as the minimum inhibitory concentration or MIC.

The minimum bactericidal concentration (MBC), or the lowest concentration of chitosan or nanoparticles that kills 99.9% of bacteria, was determined by assaying the live organisms in those tubes from the MIC test that showed no growth.<sup>20</sup> A loopful from each of those tubes were inoculated on EMB (Eosin–Methylene Blue) agar and examined for signs of growth. Growth of bacteria

demonstrates the presence of these bacteria in the original tube. On the contrary, if no growth was observed, the original tube contained no living bacteria, and the chitosan and nanoparticles were considered as being bactericidal at that concentration.

## 2.5. Atomic force microscopy

The antibacterial process of chitosan nanoparticles against *S. choleraesuis* was elucidated by AFM observation at intervals. Chitosan nanoparticles were added to bacterial cultures grown to the late exponential phase (a final concentration of 64  $\mu\text{g}/\text{mL}$ ). Samples were removed onto the surface of a piece of mica plate after 30, 60, 90, 120, and 180 min for AFM observation. AFM worked under the same conditions as described above.

## 3. Results and discussion

### 3.1. Size, zeta potential, and morphology of chitosan nanoparticles and copper-loaded nanoparticles

The preparation of chitosan nanoparticles is based on an ionic gelation interaction between positively charged chitosan and negatively charged tripolyphosphate at room temperature.<sup>11,12</sup> The chitosan nanoparticles prepared in the experiment exhibit a white powdered shape and are insoluble in water, dilute acidic and alkali solutions. The mean size and size distribution of each batch of nanoparticle suspension was analyzed using the Zeta-sizer analysis. The size distribution profile, as shown in Figure 1, represents a typical batch of nanoparticles with a mean diameter of 40 nm and a narrow size distribution (polydispersity index <1). The size of copper-loaded nanoparticles was about 257 nm as shown in Figure 2. Chitosan nanoparticles were stable under the autoclaving conditions. The particle size of autoclaved chitosan nanoparticles was determined as described above.

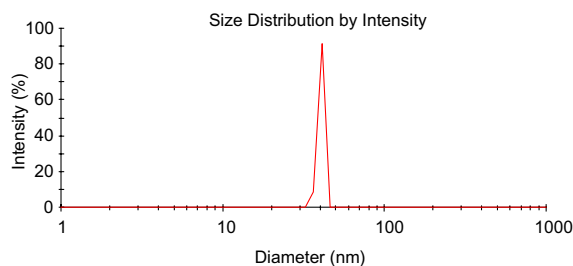


**Figure 1.** The size distribution by intensity of chitosan nanoparticles. The size of chitosan nanoparticles ranges from 28.3 to 48.7 nm, and the mean size is about 40 nm.

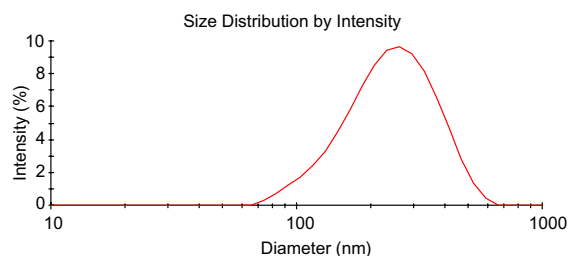


**Figure 2.** The size distribution by intensity of copper-loaded chitosan nanoparticles. The size of copper-loaded nanoparticles ranges from 65.19 to 663.8 nm, and the average size is about 257 nm.

Zeta potential, that is, surface charge, can greatly influence particle stability in suspension through the electrostatic repulsion between particles. It can also determine nanoparticle interaction in vivo with the cell membrane of bacteria, which is usually negatively charged. Figure 3 shows that the surfaces of chitosan nanoparticles have a positive charge about 51 mV, while that of copper-loaded nanoparticles exhibit about 96 mV as shown in Figure 4.

Chitosan nanoparticles as shown in Figure 5A by AFM observation exhibit a regular assemblage shape like snowflakes under pH 4.5, while the structure of the copper-loaded nanoparticles turns to an irregular shape after chelating with copper ions, and the size apparently increases as shown in Figure 5B.

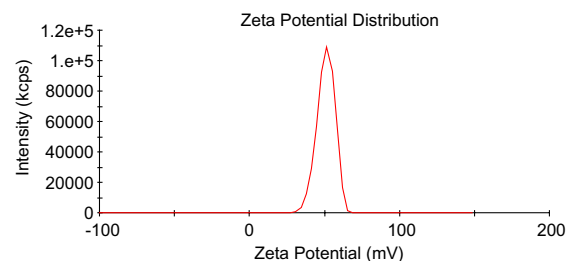


**Figure 3.** Zeta potential distribution of chitosan nanoparticles. Chitosan nanoparticles exhibit a zeta potential range from 30.8 to 68.9 mV and have a mean charge with 51 mV.

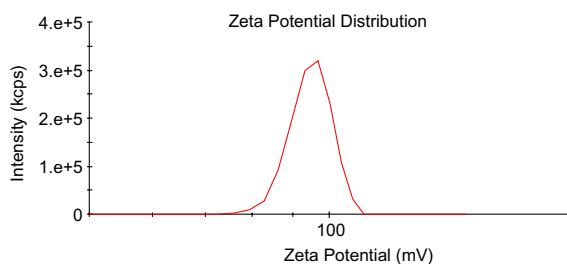


**Figure 4.** Zeta potential distribution of copper-loaded chitosan nanoparticles. Copper-loaded chitosan nanoparticles exhibit a zeta potential range from 75.9 to 110.05 mV and have a mean charge with 96 mV.

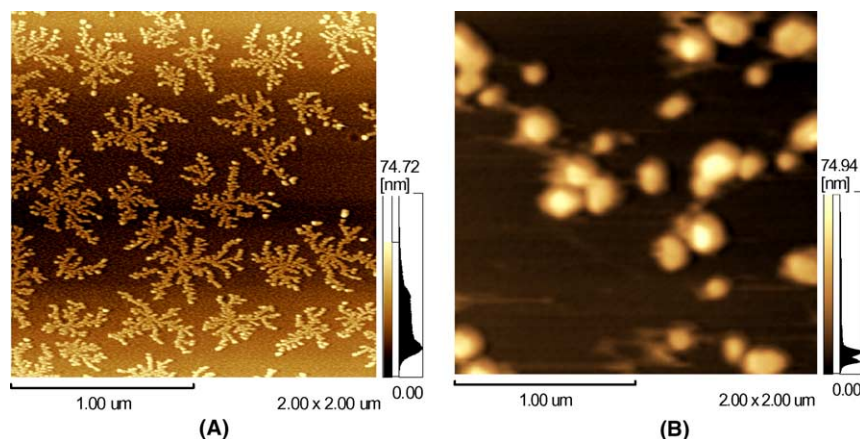


**Figure 5.** Atomic force micrographs (AFMs) of chitosan nanoparticles at pH 5.0. Chitosan nanoparticles (A), and copper-loaded nanoparticles (B).

The size, surface charge, and morphology of chitosan nanoparticles were all greatly affected by adsorbing copper ions. Chitosan nanoparticles can be considered to be microporous biopolymers; therefore, pores are large enough to let copper ions through. Copper ions are first adsorbed onto the external surface of chitosan nanoparticles, then diffuse into the small pores of nanoparticles. Finally, the ions can be chelated onto the internal surface of chitosan nanoparticles. Chitosan is a kind of polysaccharide biopolymer whose structure is well suited for the sorption of copper ions, and the sorption of ions is based in ionic exchange, complexing physical sorption by van der Waals forces and inter- or intracellular trapping.<sup>21</sup> Chitosan nanoparticles are formed through the interaction of positively charged chitosan and negatively charged tripolyphosphate. The process changes the structure and surface electric charge of chitosan due to the disruption of the secondary structure formed in its natural structure. The relatively loose structure of chitosan nanoparticles and lower crystallinity allow the organic ligands to easily interact with copper ions. The higher surface area of nanoparticles can provide more sorption sites to bind with metal ions. Therefore, chitosan nanoparticles adsorb copper ions mainly as ion-exchange resins and surface chelation. Active copper ions can also dissociate among the microporous nanoparticles. As a result, the size, surface charge, and morphology of copper-loaded nanoparticles change considerably more than those of chitosan nanoparticles without copper.

### 3.2. FTIR analysis

Chitosan nanoparticles were prepared between chitosan and tripolyphosphate. FTIR studies of chitosan, chitosan nanoparticles, and copper-loaded nanoparticles were performed to characterize the chemical structure of nanoparticles. FTIR spectra of chitosan, chitosan nanoparticles, and copper-loaded nanoparticles are

shown in **Figure 6**. A band at  $3419\text{cm}^{-1}$  corresponds to the combined peaks of the  $\text{NH}_2$  and  $\text{OH}$  group stretching vibration in chitosan. The band at  $1657\text{cm}^{-1}$  is attributed to the  $\text{CONH}_2$  group. The  $1598\text{cm}^{-1}$  peak of the  $\gamma(\text{NH}_2)$  bending vibration is sharper than the peak at  $1657\text{cm}^{-1}$ , which shows the high degree of deacetylation of the chitosan. A shift from  $3419$  to  $3427\text{cm}^{-1}$  is shown, and the peak is sharper in the chitosan nanoparticles, which indicates that the hydrogen bonding is enhanced. The intensities of ( $\text{CONH}_2$ ) band at  $1657\text{cm}^{-1}$  and ( $\text{NH}_2$ ) band at  $1598\text{cm}^{-1}$ , which can be observed clearly in pure chitosan, decrease dramatically, and two new sorption bands at  $1632$  and  $1547\text{cm}^{-1}$  appear, which shows that the ammonium groups are crosslinked with tripolyphosphate

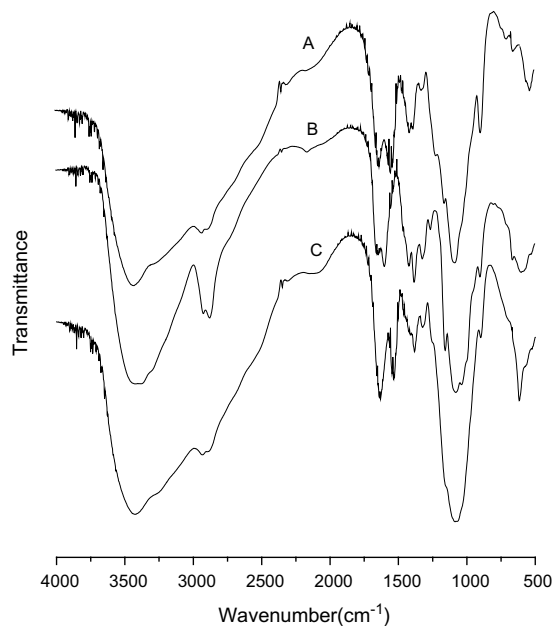


**Figure 6.** FTIR spectra. Chitosan nanoparticles (A), chitosan (B), and copper-loaded nanoparticles (C).

molecules.<sup>12</sup> Thus it is postulated that polyphosphoric groups of sodium polyphosphate interact with the ammonium groups of chitosan, which serves to enhance both the inter- and intramolecular interaction in chitosan nanoparticles. Similar results were observed in a previous study.<sup>22</sup>

Copper-loaded nanoparticles were formed by sorption of copper ions. The peaks at  $1657\text{cm}^{-1}$  ( $\text{CONH}_2$ ) and  $1598\text{cm}^{-1}$  ( $\text{NH}_2$ ) in the spectrum of copper-loaded nanoparticles are sharper and separately shift to  $1631$  and  $1536\text{cm}^{-1}$ . The  $\gamma$  ( $\text{C-N}$ ) peak at  $1421\text{cm}^{-1}$  disappears, and the  $\gamma$  ( $\text{CH}_3$ ) peak of the group acetyl at  $1380\text{cm}^{-1}$  shifts to  $1383\text{cm}^{-1}$ .  $\text{Cu(II)}$  bonding could cause the substantial redistribution of vibration frequencies in the above-mentioned region typical of different types of ( $-\text{OH}$ ,  $-\text{NH}$ ) vibrations in chitosan reported by others.<sup>23</sup> Therefore, complexation of  $\text{Cu(II)}$  with chitosan nanoparticles results in ionic bonding similar to  $\text{Cu(II)}$ -polymer bonding.

### 3.3. X-Ray diffraction (XRD) pattern of chitosan and chitosan nanoparticles

X-Ray powder diffraction patterns of chitosan, chitosan nanoparticles and copper-loaded nanoparticles are shown in Figure 7. There are two strong peaks in the diffractogram of chitosan at  $2\theta$  at  $10.4^\circ$  and  $21.8^\circ$ , indicating the high degree of crystallinity of chitosan, their crystal lattice constant  $a$  corresponding to  $8.470$  and  $4.075$ . However, no peak is found in the diffractograms of chitosan nanoparticles and copper-loaded nanoparticles. There are no differences between the diffractogram of the chitosan nanoparticles and copper-loaded nanoparticles. The XRD of chitosan is characteristic of an amorphous polymer. Chitosan nanoparticles are comprised of a dense network structure of interpenetrating polymer chains crosslinked to each other by TPP

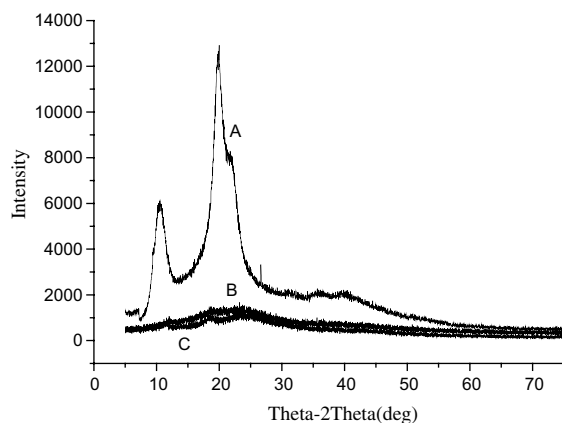


Figure 7. X-ray powder diffraction patterns of chitosan and chitosan nanoparticles. Chitosan (A), copper-loaded nanoparticles (B), and chitosan nanoparticles (C).

counterions.<sup>24</sup> The XRD implicated greater disarray in chain alignment in the nanoparticles after crosslinks.

### 3.4. Antibacterial assessment

Since chitosan is only soluble in acidic media, the precipitation of chitosan solution in acetic acid occurred upon addition to bacterial suspension, while chitosan nanoparticles could be well distributed in bacterial suspension after a slight shock for a nice dispersion. Bacteria can adhere to the surface of chitosan and chitosan nanoparticles significantly in short time of just 30 min; thus chitosan and chitosan nanoparticles exhibit antibacterial activity. According to the literature,<sup>25,26</sup> chitosan possess antimicrobial activity against a number of Gram-negative and Gram-positive bacteria. The antibacterial activity of chitosan nanoparticles and copper-loaded nanoparticles were compared with that of chitosan in distilled water or 0.25% acetic acid, respectively. Tables 1 and 2 show the MIC and MBC of chitosan, doxycycline, and chitosan nanoparticles against various microorganism in water and 0.25% acetic acid. According to these data, the antibacterial activity of chitosan nanoparticles and copper-loaded nanoparticles are significantly higher than that of chitosan and doxycycline. Furthermore, the test samples exhibit lower antibacterial activity in water compared with that of samples in 0.25% acetic acid. Moreover, the MIC and MBC values of copper-loaded nanoparticles against some bacteria are lower than those of chitosan nanoparticles, which indicate higher antibacterial activity.

### 3.5. Atomic force microscopy (AFM)

The morphology of chitosan nanoparticle-treated *S. choleraesuis* was examined by AFM. When the bacteria were treated with  $64\text{ }\mu\text{g/mL}$  of chitosan nanoparticles for 30 min, the cells were surrounded by chitosan nanoparticles. The cells were degraded from a spherical shape to irregularly condensed masses when treated for 60 min as shown in Figure 8. With a time delay, *S. choleraesuis* cells were disrupted to a considerable degree with the leakage of cytosolic components, membrane sloughing, breaching, and bleeding. Chitosan nanoparticle-treated *S. choleraesuis* cells began to fragment when treated for 3 h.

Several mechanisms for the antimicrobial action of chitosan have been postulated. There are as follows: (1) Chitosan could chelated with trace elements or essential nutrients so as to inhibit the growth of bacteria.<sup>27</sup> (2) Chitosan could interact with anionic groups on the cell surface and form polyelectrolyte complexes with bacterial surface compounds,<sup>28</sup> thereby forming an impermeable layer around the cell, which prevents the transport of essential solutes into the cell.<sup>29</sup>

**Table 1.** MIC ( $\mu\text{g/mL}$ ) and MBC ( $\mu\text{g/mL}$ ) of doxycycline solution, chitosan nanoparticles, and copper-loaded nanoparticles suspension at pH6.5 against various microorganism in distilled water<sup>a</sup>

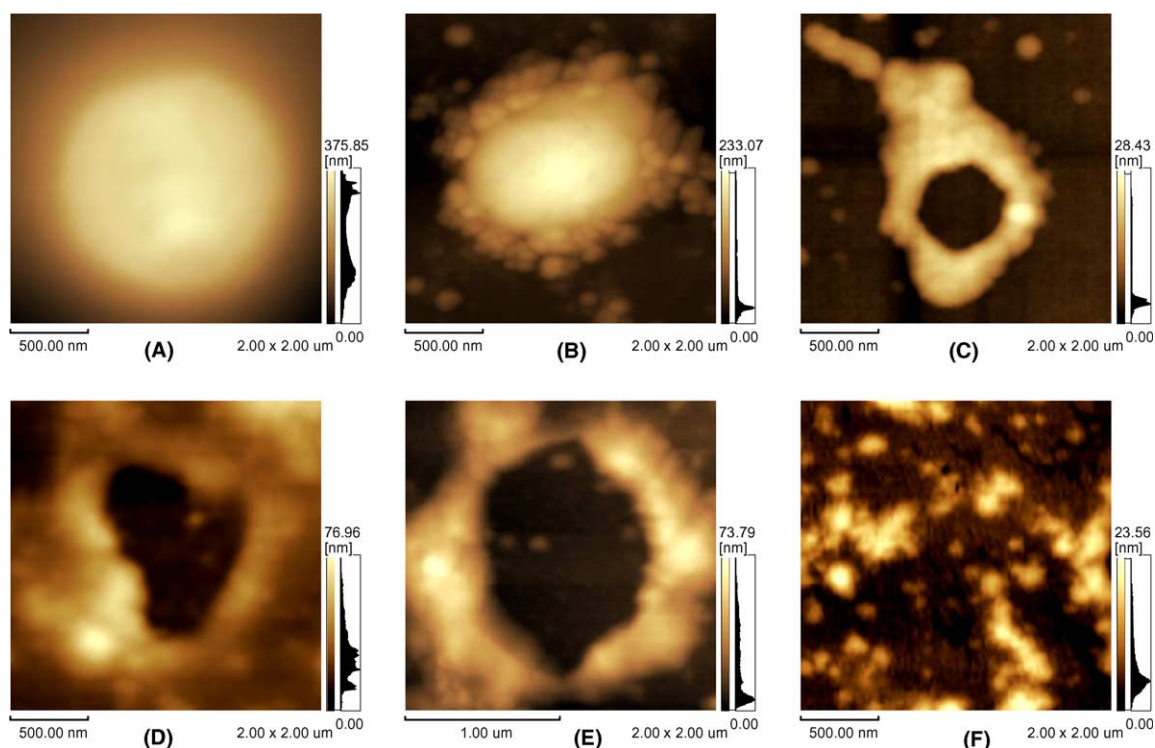
| Bacteria                          | Doxycycline |     | CNP  |     | CNP-Cu |     |
|-----------------------------------|-------------|-----|------|-----|--------|-----|
|                                   | MIC         | MBC | MIC  | MBC | MIC    | MBC |
| <i>E. coli</i> K88                | 1           | 8   | 1/8  | 4   | 1/16   | 2   |
| <i>E. coli</i> ATCC 25922         | 2           | 16  | 1/16 | 2   | 1/16   | 2   |
| <i>S. choleraesuis</i> ATCC 50020 | 4           | 32  | 1/8  | 4   | 1/16   | 2   |
| <i>S. typhimurium</i> ATCC 50013  | 4           | 64  | 1/4  | 8   | 1/8    | 4   |
| <i>S. aureus</i> ATCC 25923       | 1/4         | 8   | 1/4  | 8   | 1/8    | 4   |

<sup>a</sup> CNP = chitosan nanoparticles suspension; CNP-Cu = copper-loaded chitosan nanoparticle suspension; doxycycline = the solution of doxycycline in distilled water.

**Table 2.** MIC ( $\mu\text{g/mL}$ ) and MBC ( $\mu\text{g/mL}$ ) of chitosan solution, chitosan nanoparticles, and copper-loaded nanoparticles suspension at pH5.0 against various microorganism in 0.25% acetic acid<sup>a</sup>

| Bacteria                          | Chitosan |     | CNP  |     | CNP-Cu |     | Doxycycline |     | Control |      |
|-----------------------------------|----------|-----|------|-----|--------|-----|-------------|-----|---------|------|
|                                   | MIC      | MBC | MIC  | MBC | MIC    | MBC | MIC         | MBC | MIC     | MBC  |
| <i>E. coli</i> K88                | 8        | 64  | 1/16 | 1   | 1/32   | 1   | 1           | 4   | 2500    | 2500 |
| <i>E. coli</i> ATCC 25922         | 8        | 64  | 1/32 | 2   | 1/32   | 1   | 2           | 16  | 2500    | 2500 |
| <i>S. choleraesuis</i> ATCC 50020 | 16       | 32  | 1/16 | 2   | 1/32   | 1   | 4           | 32  | 2500    | 2500 |
| <i>S. typhimurium</i> ATCC 50013  | 16       | 64  | 1/8  | 4   | 1/16   | 2   | 2           | 32  | 2500    | 2500 |
| <i>S. aureus</i> ATCC 25923       | 8        | 32  | 1/8  | 4   | 1/16   | 2   | 1/4         | 8   | 2500    | 2500 |

<sup>a</sup> Chitosan = chitosan solution; CNP = chitosan nanoparticles suspension; CNP = copper-loaded chitosan nanoparticle suspension; doxycycline = the solution of doxycycline in 0.25% acetic acid; control = the blank tube treated just with broth and 0.25% acetic acid.

**Figure 8.** Atomic force micrographs (AFMs) of *S. choleraesuis* cells after treatment with chitosan nanoparticles suspension for different times. Nontreated cells (A); treated cells for 30min (B), treated cells for 1h (C), treated cells for 1.5h (D), treated cells for 2h (E), and treated cells for 3h (F).

Chitosan nanoparticles exhibit higher antibacterial activity than chitosan on account of the special character of the nanoparticles. The negatively charged surface

of the bacterial cell is the target site of the polycation.<sup>20</sup> Therefore, the polycationic chitosan nanoparticles with higher surface charge density interact with the bacteria

to a greater degree than chitosan itself. Chitosan nanoparticles provide higher affinity with bacteria cells for a quantum-size effect. Because of the larger surface area of the chitosan nanoparticles, nanoparticles could be tightly adsorbed onto the surface of the bacteria cells so as to disrupt the membrane, which would lead to the leakage of intracellular components, thus killing the bacteria cells.

Copper has been shown to have antibacterial properties in studies *in vivo*.<sup>30,31</sup> Copper complexes produced remarkable pharmacological effects, which are not observed when the parent ligands or inorganic forms of copper are used.<sup>32</sup> Various copper complexes have been reported to inhibit the growth of microorganisms.<sup>33,34</sup> The mode of interaction of the anion would have a great effect on the stereochemistry and the properties of the resulting metal complexes. The biological activities of metal complexes depend upon the charge, the nature of the counteranion, the geometrical configuration, and the oxidation state of the central metal ion.<sup>35</sup> The superior antibacterial activity of copper complexes compared to the free ligands can be well understood by considering chelation theory. Chelation reduces the polarity of the central metal ion, which subsequently increases the lipophilicity of the chelates and enhances their permeation through the lipid layer of the cell membrane. After penetration of the complex into the organism, the intracellular copper(II) probably undergoes reduction to a copper(I) complex by cellular oxidization. The  $\text{Cu}^+/\text{Cu}^{2+}$  couple is involved as a redox center. The  $\text{O}_2^-$  and  $\text{H}_2\text{O}_2$  produced by such redox reactions cause cytotoxic reactions by inhibition of DNA synthesis and destruction of cell viability.<sup>36</sup>

Copper-loaded chitosan nanoparticles exhibit greatly higher antibacterial activity than chitosan itself or doxycycline, and slightly higher than chitosan nanoparticles without copper. The average zeta potential of copper-loaded nanoparticles at 96 mV increases greatly from that of chitosan nanoparticles at 51 mV due to the sorption of copper ions onto chitosan nanoparticles. Therefore, the higher surface charge density of copper-loaded nanoparticles, which enhances the affinity with the negatively charged bacteria membrane, is probably responsible for their higher antibacterial activity. What is more, copper-loaded nanoparticles could possibly provide controlled release of copper ions that are dissociated in the small cores of the chitosan nanoparticles so as to exhibit continuous antibacterial activity.

#### 4. Conclusions

In summary, chitosan nanoparticles and copper-loaded nanoparticles have been synthesized and characterized in the present study. The nanoparticles obtained in the present study have small particle size and positive sur-

face charges, which may improve their stability in the presence of biological cations<sup>37</sup> and improve for their antibacterial activities due to the interaction with negatively charged biological membranes and site-specific targeting *in vivo*.<sup>38</sup> These studies show that chitosan nanoparticles and copper-loaded nanoparticles could inhibit the growth of various microorganisms markedly and exhibit higher antibacterial activity than chitosan itself or doxycycline. Their MIC values were less than 0.25  $\mu\text{g}/\text{mL}$ . AFM of chitosan nanoparticles-treated cultures of *S. choleraesuis* revealed that the antibacterial action was probably via membrane disruption and leakage of cellular protein so as to kill the bacteria cells due to the change of membrane penetrability. It is anticipated that chitosan nanoparticles could be applied broadly as antimicrobial agents in medicine for their high antibacterial activity and acceptable biocompatibilities.

#### Acknowledgement

The financial support of the Zhejiang Science and Technology Council (No. 021102680) is gratefully acknowledged.

#### References

- Kendra, D. F.; Hadwiger, L. A. *Exp. Mycol.* **1984**, *8*, 276–281.
- Sudarshan, N. R.; Hoover, D. G.; Knorr, D. *Food Biotechnol.* **1992**, *6*, 257–272.
- Tsai, G. J.; Su, W.-H. *J. Food. Protect.* **1999**, *62*, 239–243.
- Li, Zhi; Zhuang, Xu Pin; Liu, Xiao Fei; Guan, Yun Lin; Yao, Kang De. *Polymer* **2002**, *43*, 1541–1547.
- Jia, Zhishen; Shen, Dongfeng; Xu, Weiliang. *Carbohydr. Res.* **2001**, *333*, 1–6.
- No, Hong Kyoong; Park, Na Young; Lee, Shin Ho; Meyers, Samuel P. *Int. J. Food Microbiol.* **2002**, *74*, 65–72.
- Van der Lubben, I. M.; Verhoef, J. C.; Borchard, G.; Junginger, H. E. *Adv. Drug Deliver. Rev.* **2001**, *52*, 139–144.
- Roy, K.; Mao, H. Q.; Huang, S. K.; Leong, K. W. *Nature Med.* **1999**, *5*, 387–391.
- Kumar, M.; Behera, A. K.; Lockey, R. F.; Zhang, J.; Bhullar, G.; De La Cruz, C. P.; Chen, L. C.; Leong, K. W.; Huang, S. K.; Mohapatra, S. S. *Hum. Gene Ther.* **2002**, *13*, 1415–1425.
- Janes, Kevin A.; Fresneau, Marie P.; Marazuela, Ana.; Fabra, Angels; Alonso, Maria Jose *J. Control. Release* **2001**, *73*, 255–267.
- De Campos, Angela M.; Sanchez, Alejandro; Alonso, Maria J. *Int. J. Pharm.* **2001**, *224*, 159–168.
- Xu, Yongmei; Du, Yumin *Int. J. Pharm.* **2003**, *250*, 215–226.
- Pan, Yan; Li, Ying-jian; Zhao, Hui-ying; Zheng, Jun-min; Xu, Hui; Wei, Gang; Hao, Jin-song; Cui, Fu-de *Int. J. Pharm.* **2002**, *249*, 139–147.
- Mao, Hai-Quan; Roy, Krishnendu; Troung-Le, Vu L.; Janes, Kevin A.; Lin, Kevin Y.; Wang, Yan; August, J.

- Thomas; Leong, Kam W. *J. Control. Release* **2001**, *70*, 399–421.
15. Kim, Tae Hee; Park, In Kyu; Nah, Jae Woon; Choi, Yun Jaie; Cho, Chong Su. *Biomaterials* **2004**, *25*, 3783–3792.
16. Portero, A.; Remunan-Lopez, C.; Criado, M. T.; Alonso, M. J. *J. Microencapsulation* **2002**, *19*, 797–809.
17. Hu, Yong; Jiang, Xiqun; Ding, Yin; Ge, Haixiong; Yuan, Yuyan; Yang, Changzheng. *Biomaterials* **2002**, *23*, 3193–3201.
18. Qurashi, T.; Blair, H. S.; Allen, S. J. *J. Appl. Polym. Sci.* **1992**, *46*, 255–261.
19. Nester, E. W.; Anderson, D. G.; Roberts, E.; Pearshall, N. N.; Nester, M. T. *Microbiology: a Human Perspect.* **2003**, *14*, 518–521.
20. Avadi, M. R.; Sadeghi, A. M. M.; Tahzibi, A.; Bayati, Kh.; Pouladzadeh, M.; Zohuriaan-Mehr, M. J.; Rafiee-Tehrani, M. *Eur. Polym. J.* **2004**, *40*, 1355–1361.
21. Cardenas, Galo; Orlando, Parra; Edelio, Taboada *Int. J. Biol. Macromol.* **2001**, *28*, 167–174; Jeon, You-Jin; Park, Pyo-Jam; Kim, Se-Kwon. *Carbohydr. Polym.* **2001**, *44*, 71–76.
22. Knaul, J. Z.; Hudson, S. M.; Creber, K. A. M. *J. Appl. Polym. Sci.* **1999**, *72*, 1721–1731.
23. Kucherov, A. V.; Kramareva, N. V.; Finashina, E. D.; Koklin, A. E.; Kustov, L. M. *J. Mol. Catal. A. Chem.* **2003**, *198*, 377–389.
24. Tang, E. S. K.; Huang, M.; Lim, L. Y. *Int. J. Pharm.* **2003**, *265*, 103–114.
25. Ueno, K.; Yamaguchi, T.; Sakairi, N.; Nishi, N.; Tokura, S. *Adv. Chitin Sci.* **1997**, *2*, 156–161.
26. Jeon, Y. J.; Park, P. J.; Kim, S. K. *Carbohydr. Polym.* **2001**, *44*, 71–76.
27. Roller, S.; Covill, N. *Int. J. Food Microbiol.* **1999**, *73*, 672–681.
28. Muzzarelli, R. A. A.; Tarsi, R.; Filippini, O.; Giovanetti, E.; Biagini, G.; Varaldo, P. *Antimicrob. Agents Chemother.* **1990**, *34*, 2019–2033.
29. Choi, Bong-Kyu; Kim, Kwang-Yoon; Yoo, Yun-Jung; Oh, Suk-Jung; Choi, Jong-Hoon; Kim, Chong-Youl. *Int. J. Antimicrob. Agents* **2001**, *18*, 553–557.
30. Waerhaug, M.; Gjermo, P.; Rollar, G.; Johansen, J. A. *J. Clin. Periodontol.* **1984**, *11*, 176–180.
31. Cianco, S. G. *J. Dent. Res.* **1992**, *71*, 1450–1454.
32. Sorenson, J. R. *J. Chem. Brit.* **1984**, *12*, 1110–1113.
33. Antonietta Zoroddu, M.; Zanetti, Stefania; Pogni, Rebecca; Basosi, Riccardo *J. Inorg. Biochem.* **1996**, *63*, 291–300.
34. Carcelli, M.; Mazza, P.; Pelizzi, C.; Pelizzi, G.; Zani, F. *J. Inorg. Biochem.* **1995**, *57*, 43–62.
35. Das, A. K. *Medicinal Aspects of Bioinorganic Chemistry*; CBS: Shahdara, Delhi, 1990; Chapter 3 and references cited therein.
36. Ramadan, A. M. *J. Inorg. Biochem.* **1997**, *65*, 183–189.
37. Caly, P.; Remunan-Lopez, C.; Vila-Jato, J. L.; Alonso, M. *J. Colloid Polym. Sci.* **1997**, *275*, 46–53.
38. Meisner, D.; Pringle, J.; Mezei, M. *Int. J. Pharm.* **1989**, *55*, 13–15.